



CS-432 - COMPUTATIONAL MOTOR CONTROL

Case study 2 - Firing Rate Controller & Sensory Feedback

The content of this project has been written by:

Name:	SCIPER:
Julien Ferdinand Gouraud	300124
Adrien Théo Feillard	315921
Meriam Bouguecha	315185

March 6, 2025

Firing Rate Controller - No Sensory Feedback - Q3

The first part of this project was to implement the mathematical model of the carangiform swimming and the muscle activation equations. In this first part, the firing rate equations were set without the sensory feedback terms.

The video of the swimming fish for this exercise can be found in the folder `video_exercise_3`.

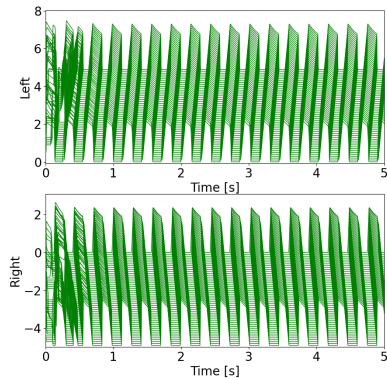
This allows us to demonstrate that the firing rate controller alone is sufficient to generate a travelling wave across the zebrafish body, leading to a proper swimming motion, which can be seen on the muscle activation graph :

For the default parameters, we obtain the following metrics :

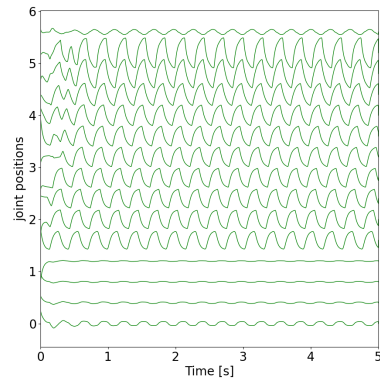
Metric	Performance
Amplitude	1.1831
Frequency	3.9952
Wave Frequency	0.7867
ptcc	1.8366
ipls	0.1969
Forward Speed PCA	0.04871
Lateral Speed	0.0011
Forward Speed Cycle	0.0485
Lateral Speed Cycle	-0.0008
Torque	0.0073
Curvature	5.6926

The observed frequency of oscillation (3.9952 Hz) falls within a realistic range for biological CPGs (1–21 Hz, with a mean of 6 Hz) validating the observed frequency as realistic (Grillner & El Manira, 2020). The amplitude (1.1831) indicates robust neural activity. The wave frequency (0.7867 Hz) aligns with the expected propagation of neural signals along the body, crucial for effective locomotion. The ptcc metric (1.8366) indicates a high degree of regularity and coordination in the oscillatory patterns, reflecting the stability of the generated rhythms. The curvature value (5.6926) suggests potential for tight maneuverability, which is vital for realistic swimming simulations.

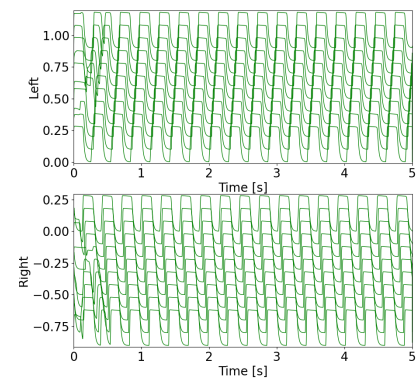
The plots of CPG activities for both left and right neurons display regular oscillations, confirming the successful generation of rhythmic patterns. The MC activity plots exhibit oscillatory patterns as well, slightly lagging the CPG activities, indicating proper signal transmission from neuron to muscles. The head trajectory plot showed a relatively straight path with minor undulations, indicating stable forward swimming with minimal lateral deviation



(a) CPG activities



(b) joint positions



(c) MC activities

In conclusion, the implementation of the firing rate controller for the zebrafish model in Exercise 3 met the expected outcomes. The generated CPG and MC activities displayed consistent and rhythmic patterns, essential for zebrafish swimming. The metrics confirmed the stability and effectiveness of the CPG network, providing a solid foundation for further exploration and integration of feedback mechanisms in subsequent exercises. These results underscore the importance and efficiency of CPG networks in generating rhythmic motor patterns.

Effect of the descending input drive I on the performance - Q4

In this part, we analyze the influence of the input drive I on the swimming motion. To put this in evidence, we perform a parameter sweep on I on the interval $[0, 30]$ with increments of 0.3 while keeping every other parameter constant.

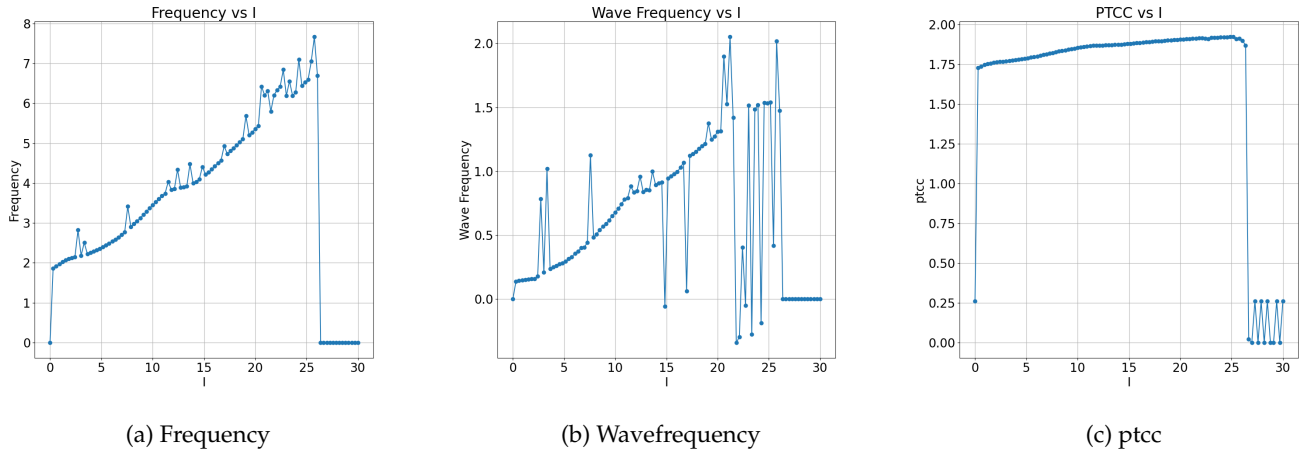


Figure 2: I parameter sweep results

Based on the results of the simulation, this are our observations:

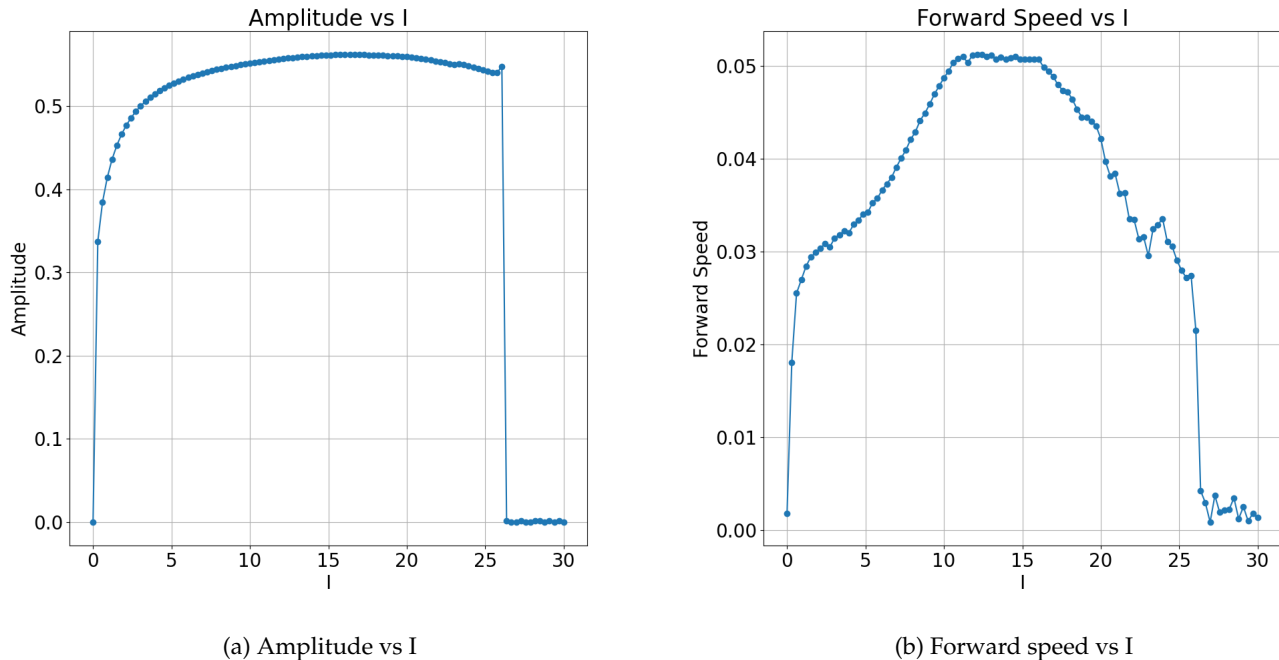
- **Stable Oscillations Range:** the CPG network supports stable oscillations for I values $\in]0;25]$. Within this range, the frequency and wave frequency increase with I , while the PTCC remains high, indicating strong and regular oscillatory patterns.
- **Frequency and Wave Frequency:** both metrics increase with I , reflecting a more rapid propagation of neural signals as the input drive strengthens. This is consistent with the expected behavior where increased input leads to higher neural activity and faster oscillations.
- **Loss of Stability:** the sharp drops in frequency, wave frequency and PTCC beyond $I=25$ indicate a loss of stable oscillatory behavior. This suggests a threshold beyond which the network dynamics can no longer support coordinated oscillations, likely due to overstimulation.

We were also curious to know the impact of I on the amplitude and the forward speed as they can give more insight on the swimming performance and robustness.

Amplitude: The amplitude increases with I and reaches a plateau, indicating that beyond a certain point, further increases in I do not significantly enhance the oscillation strength. The sharp decline beyond $I=25$ suggests overstimulation, leading to a loss of coordinated activity.

Forward Speed: The forward speed initially increases with I , peaking around $I=15$. This suggests that moderate levels of I enhance swimming performance by increasing the frequency and amplitude of the oscillations. The decline in forward speed beyond $I=15$ and the sharp drop beyond $I=25$ indicate that excessive input disrupts the coordination needed for effective locomotion.

In conclusion, the CPG network supports stable oscillations for I values between 2 and 25. Moderate I values (up to 15) enhance performance, while excessive I (beyond 25) leads to instability. These findings highlight the role of I in regulating rhythmic motor patterns in zebrafish.



Swimming Behavior and Turning Capabilities - Q5

Here, we analyze the impact of the differential input current I_{diff} . To simulate this, we incorporated the term I_{diff} directly into the firing rate controller equations. The goal is to accurately replicate the turning behavior of the zebrafish. I_{diff} represents the differential input applied to the CPG network, creating an excitation difference between the left and right sides. By adding I_{diff} to the excitation terms, we introduce asymmetry in the neural activation patterns, resulting in a turning motion. This adjustment ensures that the model accurately reflects the physiological response to differential neural inputs, allowing us to study the effects of turning in detail.

The modified equations are as follows:

1. Equation for the left CPG neuron (\dot{r}_L):

$$\tau \dot{r}_L = -r_L + F \left(I + I_{diff} - ba_L - g_{in} W_{in} \cdot r_R \right)$$

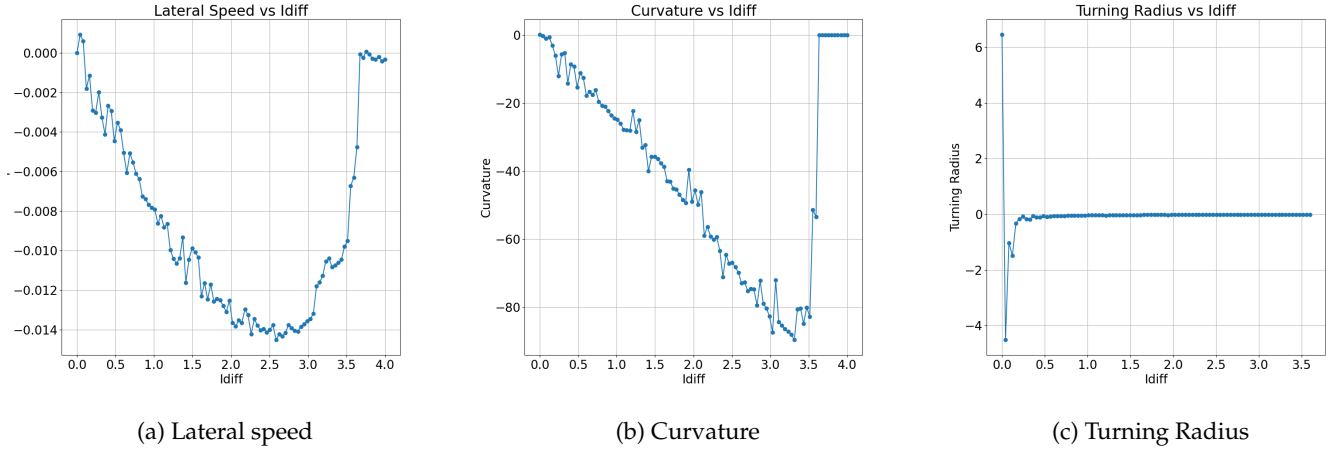
- ## 2. Equation for the right CPG neuron (\dot{r}_R):

$$\tau \dot{r}_R = -r_R + F \left(I - I_{diff} - ba_R - g_{in} W_{in} \cdot r_L \right)$$

The impact of the magnitude of I_{diff} can be analysed similarly to the impact of I , by performing a parameter sweep on the interval $[0, 4]$ with increments of 0.04. To understand the performance of each simulation, we look at the curvature of the motion as well as the lateral speed.

Varying the value of I_{diff} had a strong impact on the turning radius, curvature, and lateral speeds.

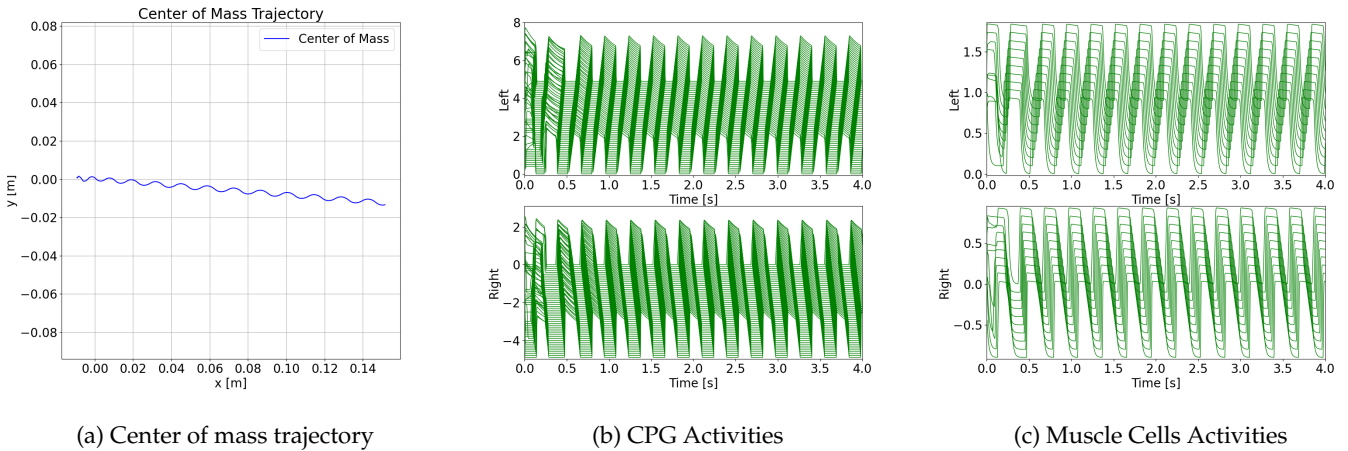
Turning Radius vs I_{diff} The turning radius plot demonstrates that as I_{diff} increases, the turning radius initially becomes more negative, indicating tighter turns. This trend continues up to around $I_{\text{diff}} = 1.5$, beyond which the turning radius stabilizes. This suggests that further increases in I_{diff} have a diminishing effect on the turning tightness, possibly due to the saturation of the control input. The convergence of the turning radius to zero implies that the fish is capable of executing extremely tight turns, effectively pivoting around a point. This behavior indicates that the zebrafish model can make sharper turns up to a certain threshold of I_{diff} , after which the turning efficiency drops.

Figure 4: I_{diff} parameter sweep results

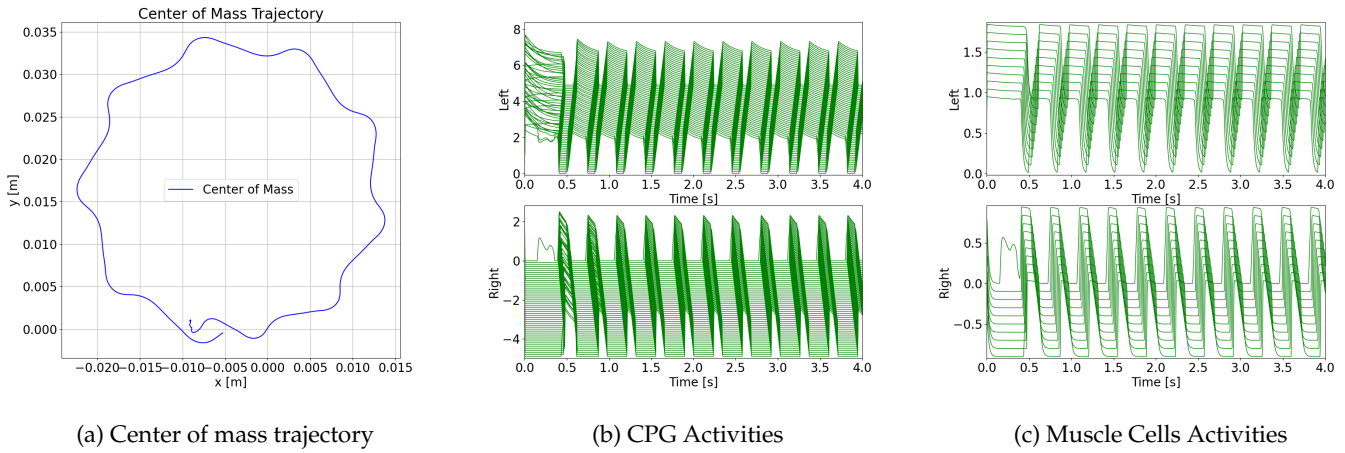
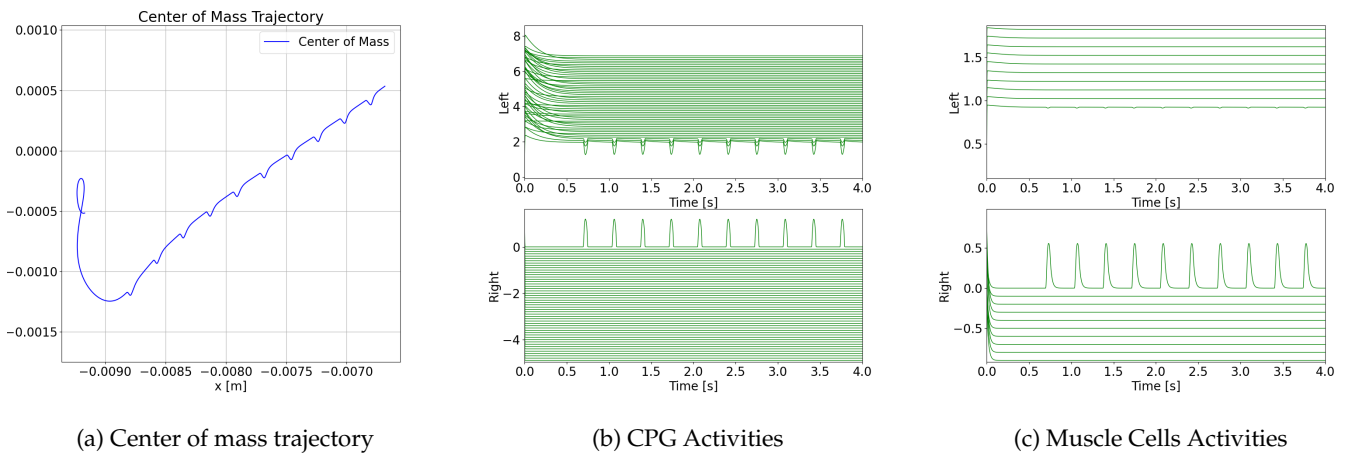
Curvature vs I_{diff} The curvature plot aligns with the observations from the turning radius. As I_{diff} increases, the curvature becomes more negative, indicating tighter turns. Similar to the turning radius, the curvature stabilizes beyond a certain I_{diff} , confirming the model's response to differential input and indicating a saturation point. This consistency across metrics reinforces the reliability of the observations.

Lateral Speed vs I_{diff} The lateral speed plot shows a significant decrease in lateral speed with increasing I_{diff} up to around $I_{\text{diff}} = 2.5$, indicating that the fish is turning more sharply and thus reducing its forward speed. However, beyond this point, there is a sharp increase in lateral speed, suggesting a change in the turning dynamics or potential instability in the control mechanism at high differential drives. This behavior underscores the importance of optimizing I_{diff} to balance turning efficiency and forward propulsion.

To further understand the impact of I_{diff} , we plotted the neuron activity and the center of mass trajectory for $I_{\text{diff}} = 0$ and $I_{\text{diff}} = 2$.

Figure 5: $I_{\text{diff}} = 0$

$I_{\text{diff}} = 0$: the center of mass trajectory shows a relatively straight path with minor lateral undulations, indicating forward swimming with minimal turning. The CPG activities are symmetric on both sides, exhibiting rhythmic oscillations with similar amplitudes and frequencies, which support balanced muscle contractions and forward propulsion.

Figure 6: $I_{diff} = 2$ Figure 7: $I_{diff} = 3.7$

$I_{\text{diff}} = 2$: the center of mass trajectory forms a circular path, reflecting the turning motion induced by moderate asymmetry in neural activation. The left CPG neurons display higher amplitude oscillations compared to the right, resulting in phase differences that drive controlled turns. Consequently, the left muscle cells exhibit higher activity levels, correlating with the increased neural input, which produces asymmetrical muscle activation and effective turning.

$I_{\text{diff}} = 3.7$: the trajectory becomes highly curved with sharp and frequent turns, indicating strong differential input. The left CPG neurons show significantly higher amplitude and more frequent oscillations than the right, creating a pronounced asymmetry that leads to vigorous muscle contractions on one side. This results in sharp and frequent turns, as reflected in the highly curved center of mass trajectory. The pronounced difference in muscle activations highlights the model's ability to produce complex locomotor patterns through strong differential input, demonstrating the importance of neural asymmetry in achieving efficient turning behavior in the zebrafish model.

Conclusions I_{diff} is a critical parameter introduced to create asymmetry in the CPG outputs, thereby inducing turning behavior in the zebrafish model. By testing and analyzing our model's response to varied I_{diff} values, we demonstrated how differential input modulates the neural and muscle activities to achieve controlled turning.

Firing Rate Controller with Sensory Feedback - Q6

We now include proprioceptive stretch feedback in our model, through the firing rate differential equations.

In this exercise, we explore the impact of sensory feedback, specifically the stretch feedback (g_{ss}), on the zebrafish model's locomotion. By analyzing the CPG activities, sensory neuron activities, muscle activities, and joint positions for $g_{ss} = 0$ and $g_{ss} = 6$, and performing a parameter sweep with $g_{ss} \in [0, 15]$, we aim to understand how sensory feedback influences swimming dynamics and control.

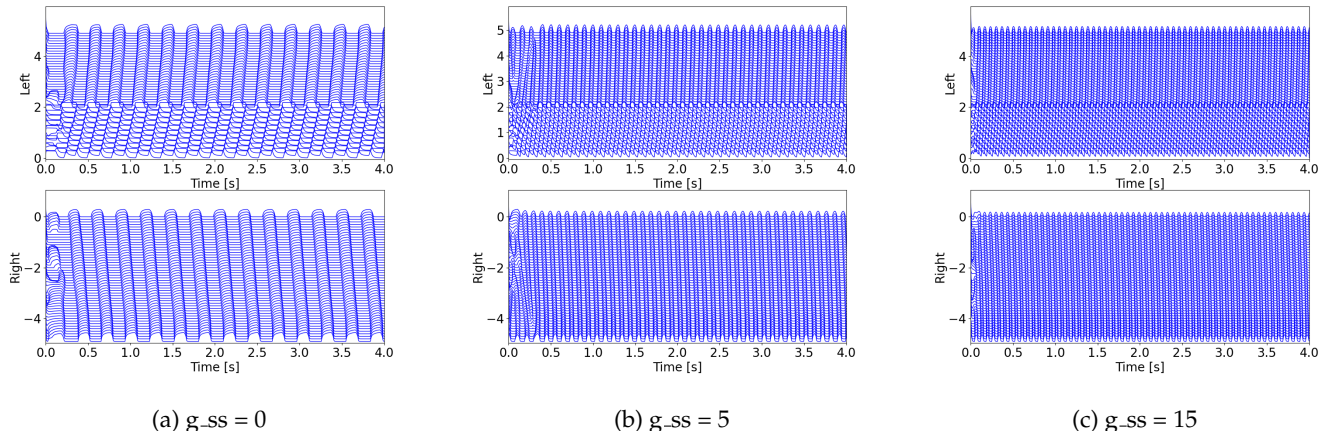


Figure 8: Sensory Neurons Activity

Center of Mass Trajectory: For $g_{ss} = 0$, the center of mass trajectory is linear and smooth, indicating stable but less dynamic propulsion. With $g_{ss} = 5$, the trajectory extends further and remains linear, showing more effective propulsion and higher speed. This optimal feedback enhances coordination and movement efficiency. However, for $g_{ss} = 15$, the trajectory becomes irregular and less extended, indicating instability and reduced efficiency due to excessive feedback causing erratic movements.

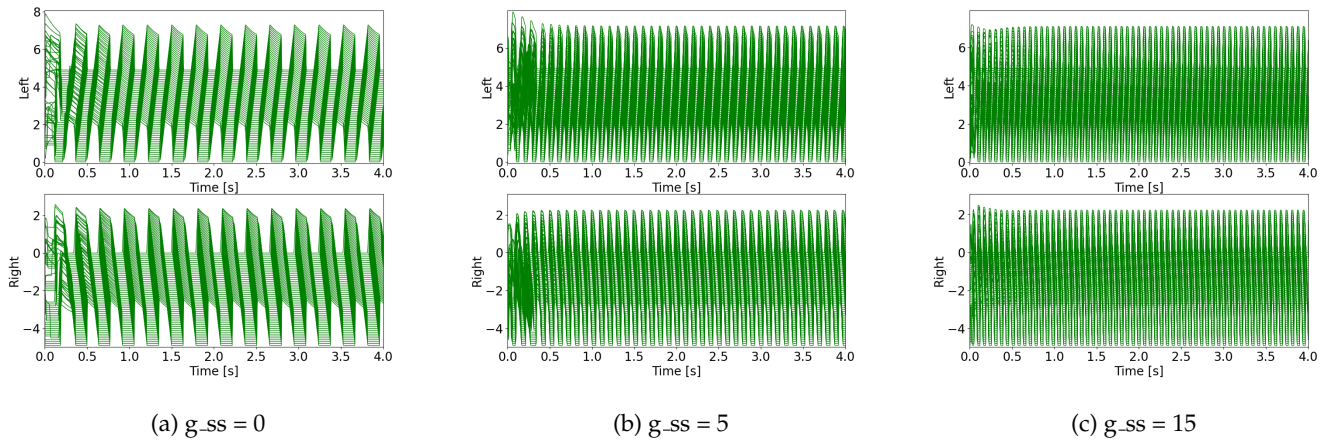


Figure 9: CPG Activity

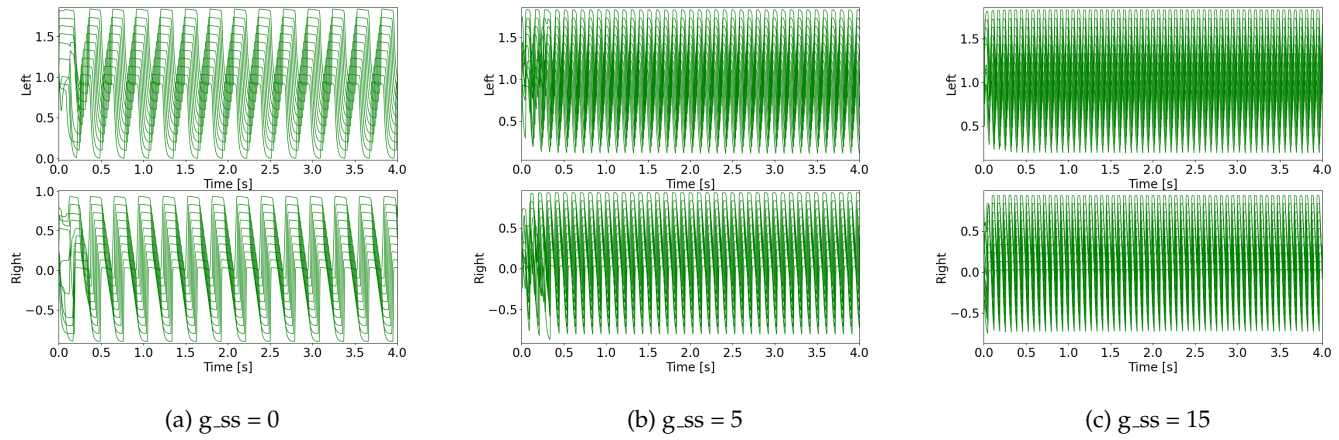


Figure 10: MC Activities

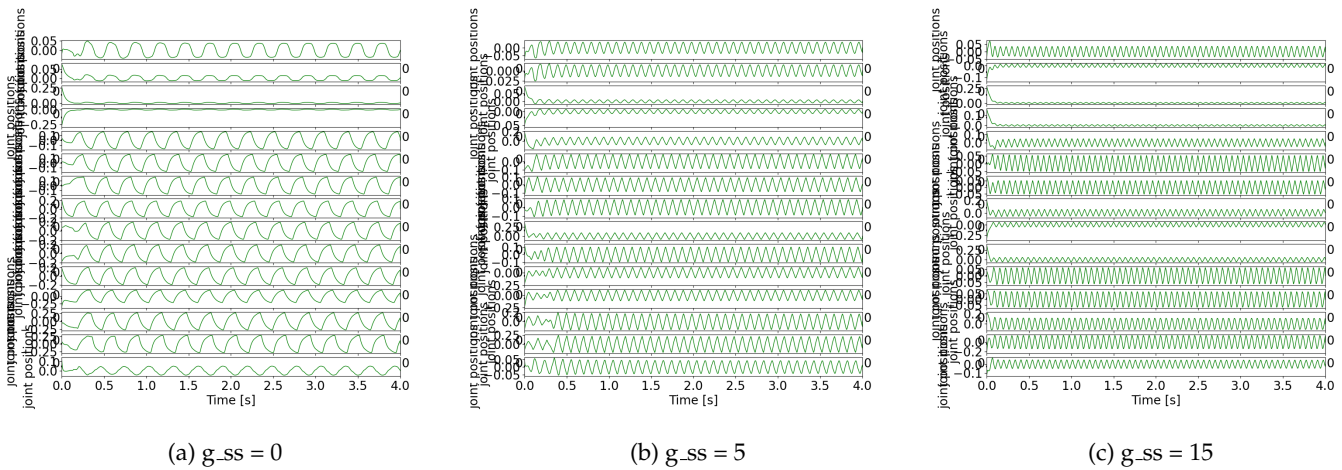


Figure 11: Joint Positions

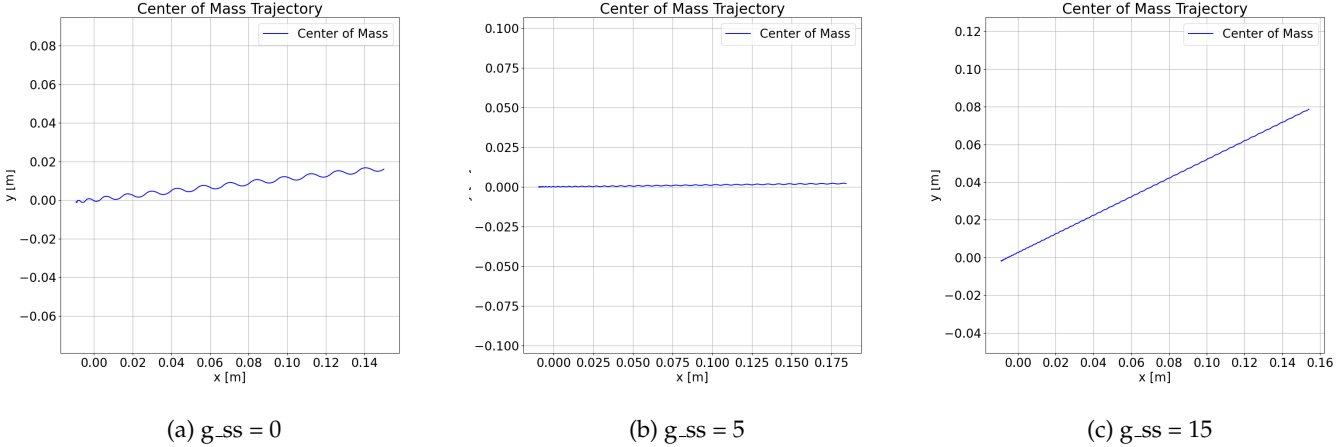


Figure 12: Center of MAss Trajectory

CPG Activities: At $g_{ss} = 0$, CPG activity is consistent but has a lower amplitude, reflecting stable neural activation without feedback enhancement. In contrast, $g_{ss} = 5$ results in higher amplitude and more regular CPG activity, indicating stronger and more consistent neural signals for efficient swimming. Conversely, $g_{ss} = 15$ causes highly variable and less regular CPG activity, with excessive feedback leading to erratic neural patterns and disrupted muscle coordination.

Joint Positions: For $g_{ss} = 0$, joint positions are stable but exhibit lower amplitude movements, indicating predictable but less dynamic motion. At $g_{ss} = 5$, joint positions show higher amplitude and regular oscillations, enhancing swimming efficiency with vigorous and coordinated movements. However, $g_{ss} = 15$ results in erratic joint positions with variable amplitudes, leading to unpredictable and inefficient swimming due to excessive feedback.

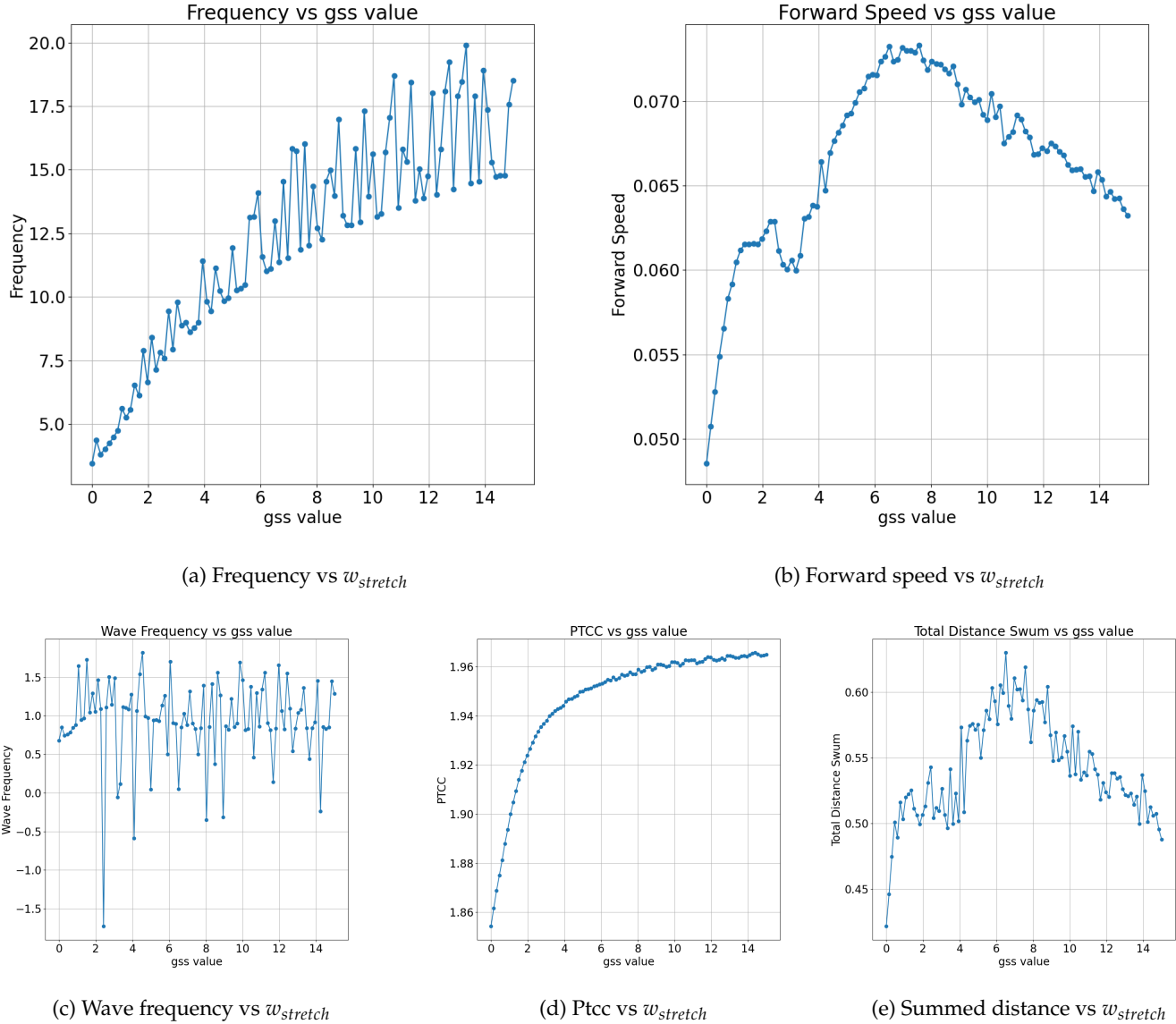
MC Activities: At $g_{ss} = 0$, MC activities are stable but show lower activation levels, reflecting basic motor command activation without feedback enhancement. With $g_{ss} = 5$, MC activities are higher and more consistent, enhancing motor commands for powerful and efficient swimming. Conversely, $g_{ss} = 15$ causes erratic and less consistent MC activities, disrupting stable motor command activation and leading to inefficient muscle movements due to excessive feedback.

Wave Frequency vs g_{ss} : As g_{ss} increases from 0 to 15, wave frequency shows considerable fluctuations. At lower g_{ss} values, the wave frequency remains relatively stable. Around $g_{ss} = 5$, the wave frequency achieves a more consistent and regular pattern, indicating optimal performance. However, as g_{ss} increases beyond this point, the wave frequency becomes increasingly erratic, suggesting instability with high feedback levels.

Total Distance Swum vs g_{ss} : The total distance swum increases with g_{ss} up to a peak around $g_{ss} = 6$. This suggests that moderate feedback enhances swimming efficiency. Beyond this point, the distance swum decreases, indicating that excessive feedback reduces performance. At $g_{ss} = 15$, the distance swum drops significantly, confirming that too much feedback is detrimental.

PTCC vs g_{ss} : PTCC steadily increases with g_{ss} and stabilizes at higher values. This shows that the number of cycles between peaks and troughs becomes more regular as feedback increases, but the impact on overall swimming efficiency depends on other factors like wave frequency and total distance.

Frequency vs g_{ss} : Frequency increases linearly with g_{ss} . At $g_{ss} = 5$, the frequency is optimal, showing a high and stable oscillation rate. As g_{ss} continues to increase, the frequency becomes less stable, indicating that high feedback can lead to overcompensation and instability in movement.

Figure 13: Parameter Sweep Results for $w_{stretch}$

Forward Speed vs g_{ss} : Forward speed increases with g_{ss} up to a peak at around $g_{ss} = 5$, reflecting optimal propulsion and efficiency. Beyond this point, the forward speed declines, showing that excessive feedback hampers effective forward motion.

Conclusions The parameter sweep results show that moderate feedback gain ($g_{ss} \approx 5$) significantly enhances zebrafish locomotion by optimizing wave frequency, total distance swum, PTCC, oscillation frequency, and forward speed. These findings align with previous analyses where $g_{ss} = 5$ produced the most efficient and stable swimming patterns. Conversely, low feedback ($g_{ss} = 0$) leads to stable but less dynamic performance, and high feedback ($g_{ss} = 15$) causes instability and reduced efficiency. This demonstrates that properly tuned feedback is crucial for maximizing swimming performance and maintaining stability in the zebrafish model.

Effect of g_{ss} on different input currents - Q7

We have now seen that the addition of the stretch feedback term can improve the performance when the zebrafish swims forward.

To understand if the impact of g_{ss} varies for different input currents, we perform a double parameter sweep, varying $I \in [0,30]$ and $g_{ss} \in [0, 15]$ over 10 values for each parameter.

When applying a differential input current with an added stretch feedback, the muscle activity is less responsive to the turning motion as the feedback tries to rectify the change in input. 14 shows that, as a constant I and I_{diff} are applied, a greater g_{ss} leads to a straighter trajectory, in the stable case ($I < 27$). This statement is also reflected by figure 19.

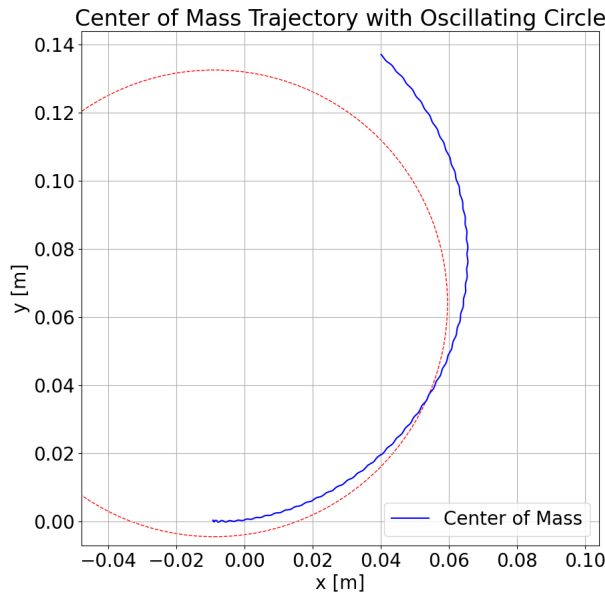
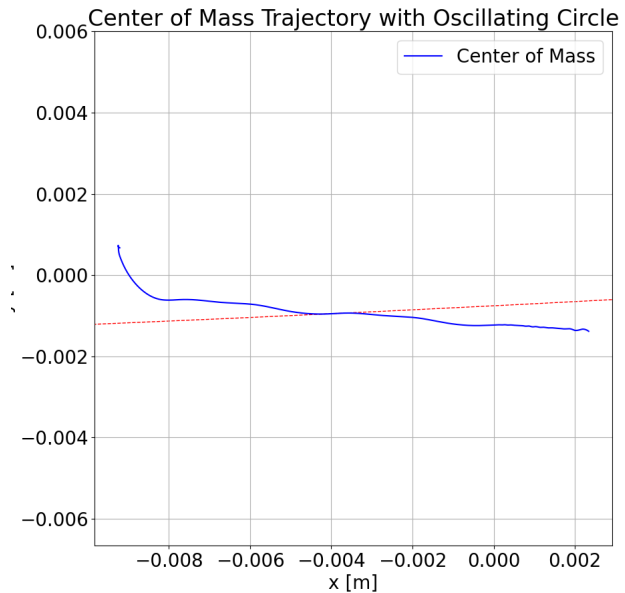
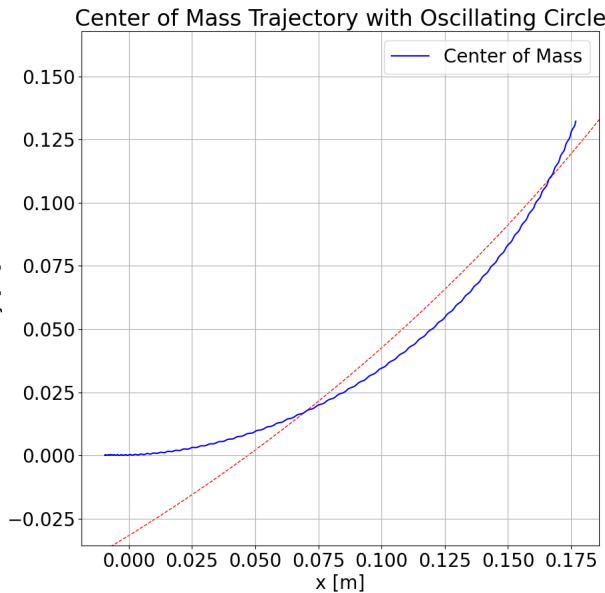
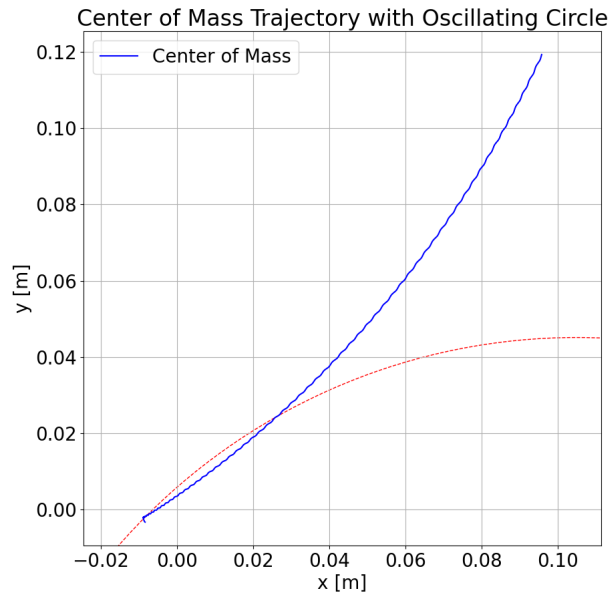
Figure 18 shows that for $I_{diff} = 0;2;4$, the frequency increases when g_{ss} increases and when I decreases.

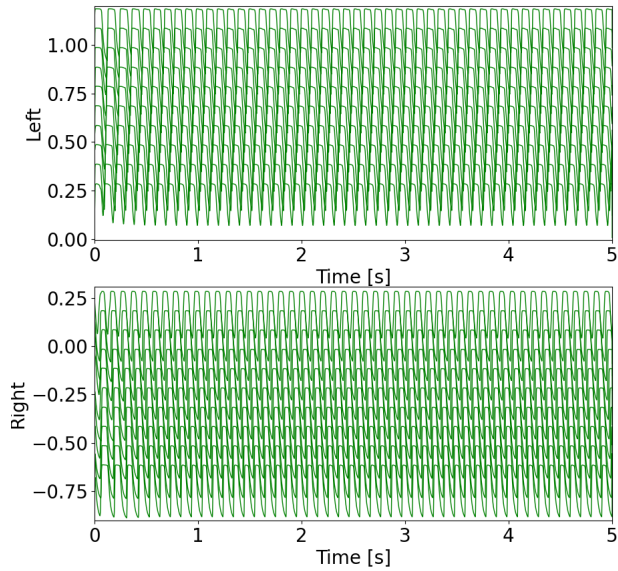
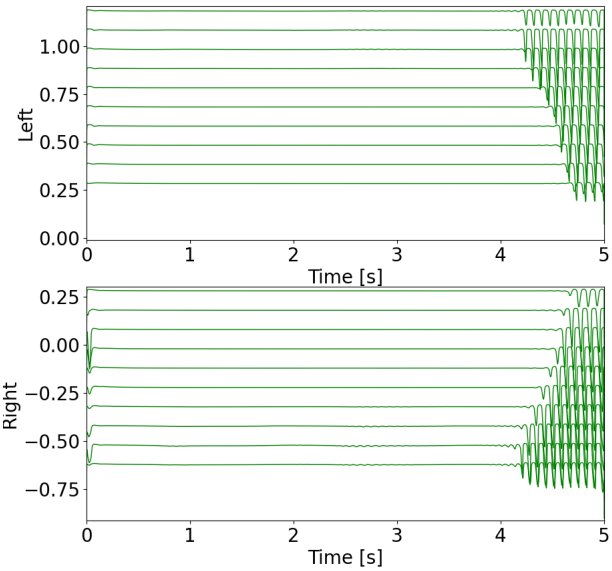
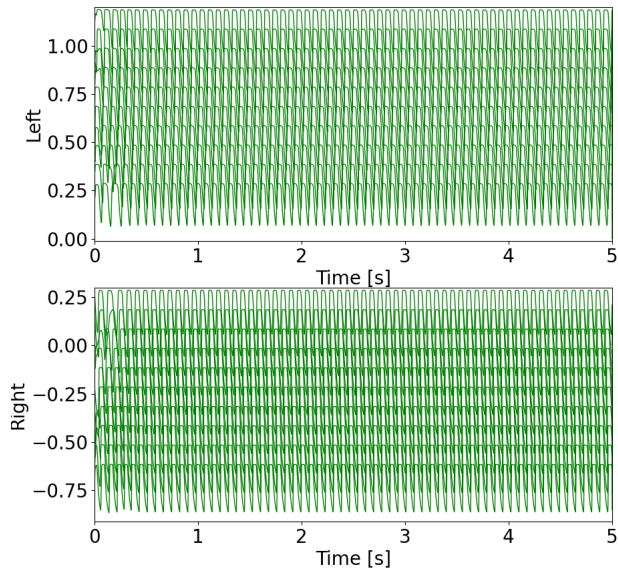
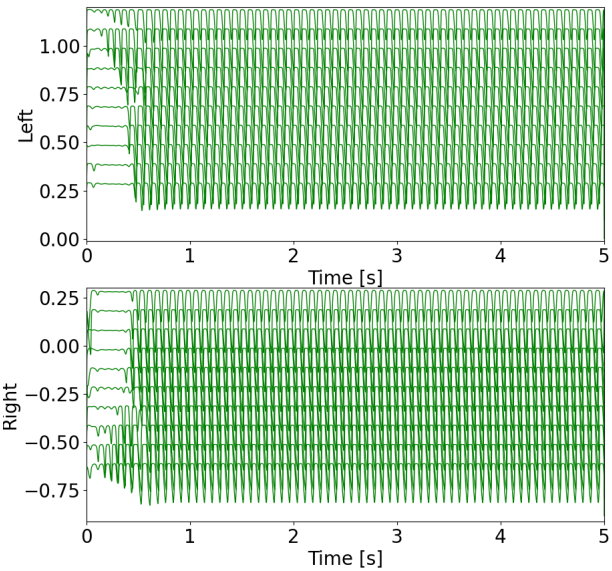
Figure 22 shows that for $I_{diff} = 0$, the wave frequency seems to increase for low g_{ss} values and high I values and decrease for high g_{ss} values and low I values^{23a}. For $I_{diff} = 2$, no patterns are discernible. The highest wavefrequency is at $g_{ss} = 10.0$ and $I = 13.3$ and the lowest wavefrequency is located at $g_{ss} \in \{10.0 ; 16.7 ; 20.0\}$ and $I \in \{5.0 ; 8.3 ; 0.0\}$ respectively. for $I_{diff} = 4$ it makes no sense to analyze to wavefrequency as the signals are unstable.

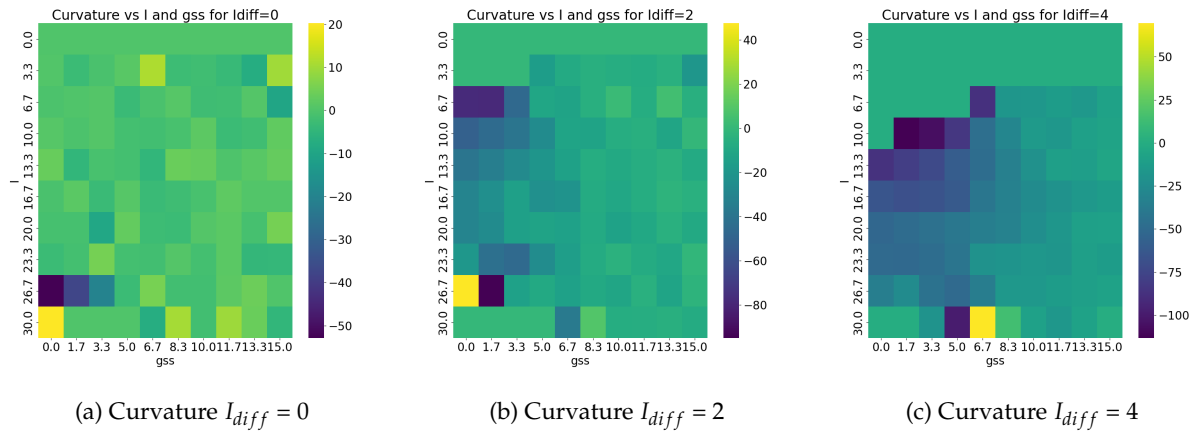
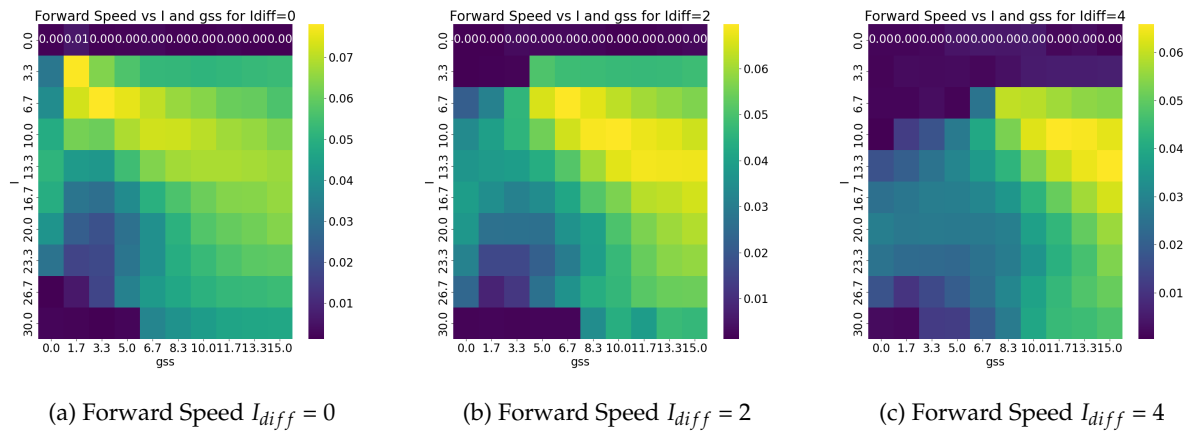
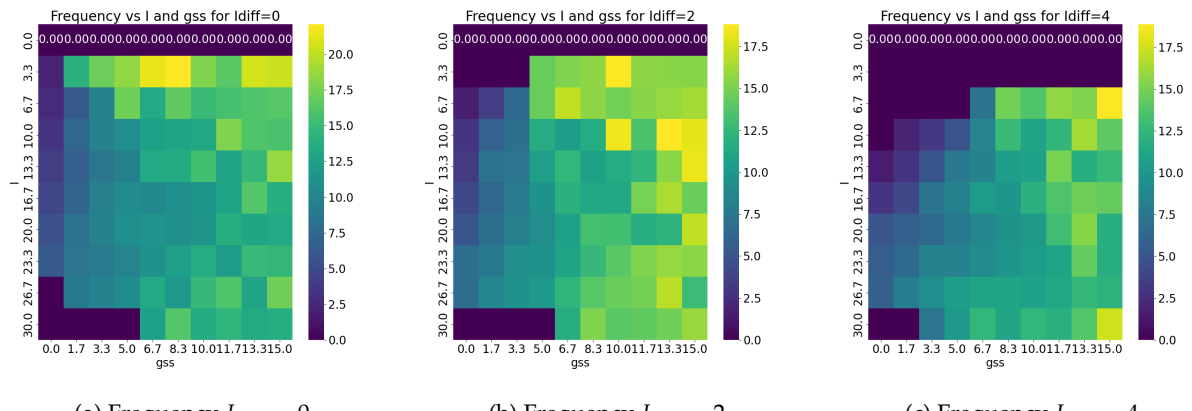
Figure 23 shows that for $I_{diff} = \{0;2;4\}$, the signals remains stable for high g_{ss} values and I values. However for high g_{ss} values low I values $\neq 0$ the signals manage to remain stable. According to Q4 2c, for I values $\in]0,25]$ the signals remains stable. This statement doesn't seems to contrast with the results²³ as the range of stability seems to decrease depending on I diff and not on g_{ss} values.

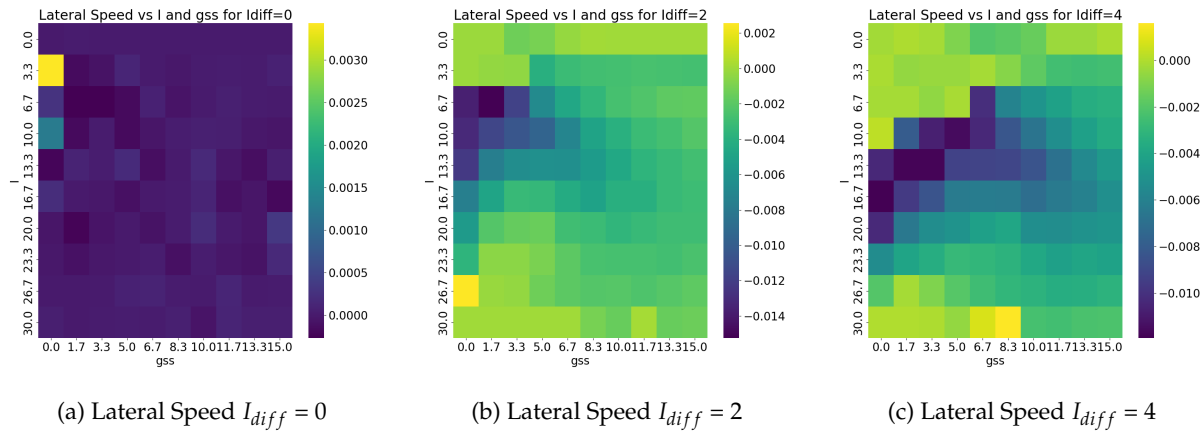
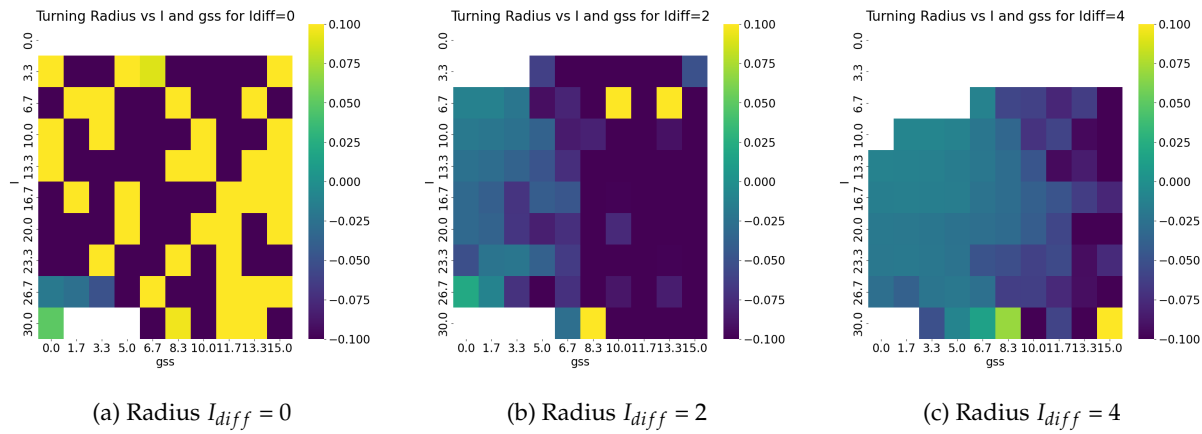
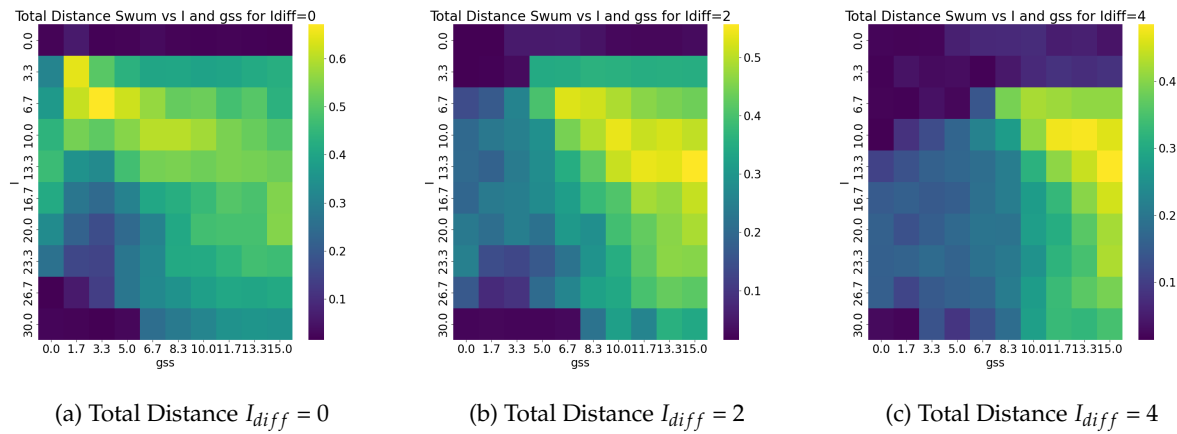
Figure 21 and 17 displays the performance of the zebrafish. They are fairly similar, which is expected. It displays that, the optimal performance range change in function of I_{diff} , I and g_{ss} . For $I_{diff} = 0$ 17a the optimal PCA forward speed seems to be reached when $I = 3.3$ and $g_{ss} = 1.7$, for $I_{diff} = 2$ 17b it seems to be reached when when $I = 6.7$ and $g_{ss} = 6.7$ and for $I_{diff} = 4$ 17c it seems to be reached when when $I = 10.0$ and $g_{ss} = 11.7$. It seems the the optimal performance follows a specific rate between I values and g_{ss} values with a rate between 0.85 and 1.95 for all I_{diff} values tested. When the values of I are in respect of this rate the optimal PCA forward speed is the same as the one from Q6 12b and higher than the model with the defaults parameters displayed in the table of Q1 (more than 0.070 vs 0.048).

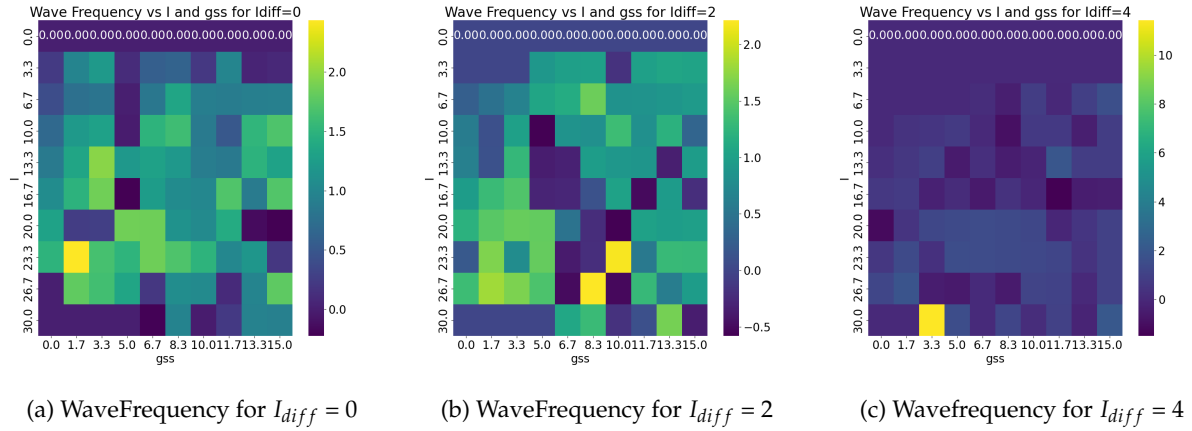
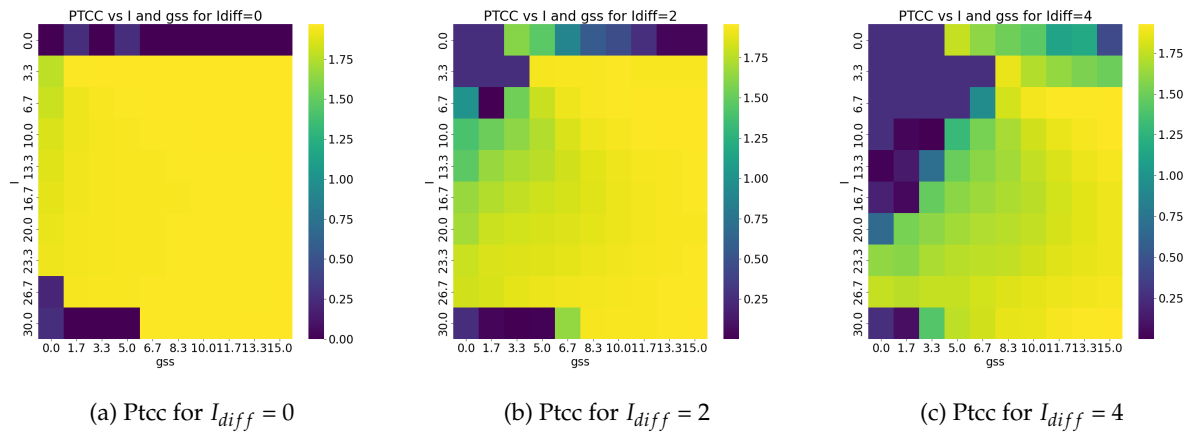
Overall, stretch feedback is very beneficial for forward spinning motion, but relying more heavily on it would be detrimental to the overall behaviour of a real fish, as it would prevent efficient target tracking and avoiding any obstacles.

(a) $I = 16.7, g_{ss} = 6.7$ (b) $I = 30.0, g_{ss} = 6.7$ (c) $I = 16.7, g_{ss} = 15.0$ (d) $I = 30.0, g_{ss} = 15.0$ Figure 14: Center of mass trajectory for $I_{diff} = 2$

(a) $I = 16.7, g_{ss} = 6.7$ (b) $I = 30.0, g_{ss} = 6.7$ (c) $I = 16.7, g_{ss} = 15.0$ (d) $I = 30.0, g_{ss} = 15.0$ Figure 15: Muscles activities for $I_{diff} = 2$

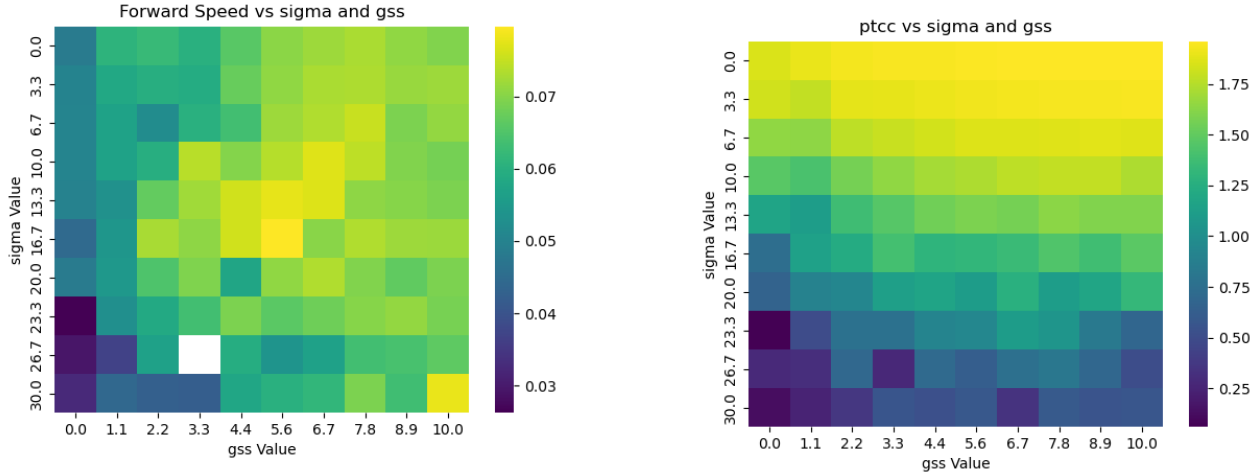
Figure 16: Curvature vs I in function of g_{ss} Figure 17: Forward Speed vs I in function of g_{ss} Figure 18: Frequency vs I in function of g_{ss}

Figure 19: Lateral Speed vs I in function of g_{ss} Figure 20: Radius vs I in function of g_{ss} Figure 21: Total Distance vs I in function of g_{ss}

Figure 22: Wavefrequency vs I in function of g_{ss} Figure 23: Ptcc vs I in function of g_{ss}

Stretch Feedback for Noise Rejection -Q8

A major advantage of stretch feedback is its ability to adapt the swimming motion to partially reject external disturbances. To visualise this, we performed a 2 parameter sweep over both σ and g_{ss} .



(a) Heatmap of the Forward speed PCA for different σ and g_{ss} values

(b) Heatmap of the ptcc value for different σ and g_{ss} values

Figure 24: Results of the parameter sweep for σ and g_{ss} values

Figure 24b shows the signals tends to be more stable the lower σ values are and when there is higher g_{ss} values. Figure 24a displays that the model reach an optimal forward PCA speed when the g_{ss} value is around 5.6 and the σ value is around 16.7

The results clearly shows the necessity of a sensory feedback to manage noise that typically happens in real. Without any feedback ($g_{ss} = 0$) the signal instability increase as the noise increase. The performance gets poorer as the forward speed is significantly lowered as the noise increases.

Open questions - Q9

During the project, you tested the effect of proprioceptive sensory feedback with varying levels of noise. How would you design a biological experiment to validate in-vivo the simulation results?

In order to validate the results of the simulation, we would need to test the swimming performance of a population of zebrafish under different levels of noise in the stretch sensory feedback.

Inducing noise in the stretch sensory feedback can be done in different ways :

- Micro-manipulators on the zebrafish muscles can apply controlled noise to the stretch feedback system.
- Specific drugs can affect muscle activity, inducing noise whose level depends on the drug dosage.

The performance of the zebrafish swimming motion under various levels of noise can then be assessed and compared with our simulation results.

What other aspects of zebrafish locomotion could be affected by the presence (or absence) of proprioceptive sensory feedback? How would you test those hypotheses in simulation and biological experiments?

In the project, we evaluated the performance of the zebrafish model with stretch feedback, but many aspects of a real-life fish behaviour can be influenced by stretch feedback :

Swimming through currents

Without stretch feedback, the muscle activations would stay the same whether the water was moving or not, resulting in erratic behaviour when the fish enters a stream. Stretch feedback helps the fish to adjust the muscle activations to adjust to a change in the environment (entering a water current).

- **Simulation :** Introduce moving water in the simulation environment, and compare the swimming performance of the models with and without stretch feedback, and understand how the strength of the feedback impacts the swimming motion.
- **Biological experiment :** Disrupt the stretch feedback of a population of zebrafish using drugs, and look at the ability of the fishes to swim under different water currents.

Avoiding obstacles

The importance of descending modulation in a zebrafish is relatively small, meaning that without any type of sensory feedback, it would struggle in obstacle avoidance as the descending modulation would not sufficiently change the muscle activation.

- **Simulation :** Simulate an environment with obstacles, and look at the ability of the model to avoid them under different levels of stretch feedback strength.
- **Biological Experiment :** Disrupt the stretch feedback of a population of zebrafish using drugs, and look at the ability of the fishes to navigate in an environment filled with obstacles.

What other types of sensory feedback could play a role during zebrafish locomotion? How would you disambiguate the relative contribution of the different sensory feedback modalities? How can simulation help in addressing this problem?

The visual and vestibular feedback are very important types of feedback that can impact the swimming behaviour and performance of the zebrafish.

To understand the impact of one of feedback, we would need to selectively block the input of the others using different techniques :

- **Visual feedback :** In order to stop visual feedback, we would need to either cover the eyes of the zebrafish, or make the zebrafish swim in the dark. This would limit or completely stop the visual feedback, but might cause the fish to stop swimming as it would lack a target to reach.
- **Vestibular feedback :** Targeting the vestibular feedback can be achieved in the same was as the stretch feedback, by injecting inhibitory drugs in the zebrafish. However, this would most likely lead to perturbation in the stretch feedback as well, meaning that we would not be able to disambiguate the two. In order to isolate the vestibular technique without impairing the stretch feedback, we would need to breed zebrafish with vestibular deficiency and selectively breed them for several generations until the vestibular feedback is completely absent. This would pose both ethical problems and time-related constraints.

This is where the simulations would really shine, as it would be extremely simple to disambiguate each type of feedback.

Once a complete model with every type of feedback has been implemented, we would only need to set the corresponding terms to 0 in order to effectively block a single type of feedback.

References

- Roth, E., & Ziegler, H. (2010). Proprioception and Motor Control: Noise and Time Delays in Muscle Receptors. *Journal of Neurophysiology*, 103(4), 1642-1655.
- Bajema, M., van Leeuwen, J. L., & van Ooyen, A. (2022). Modeling multi-sensory feedback control of zebrafish in a flow. *PLOS Computational Biology*, 18(6), e1009180.